High-Throughput Screening (HTS) of Anticancer Drug Efficacy on a Micropillar/Microwell Chip Platform

Article *in* Analytical Chemistry · November 2013

DOI: 10.1021/ac402546b · Source: PubMed

9 authors, including:

D. Lee
Korea Advanced Institute of Science and Technol…
2,021 PUBLICATIONS **16,758** CITATIONS
SEE PROFILE

Moo-Yeal Lee
Cleveland State University
53 PUBLICATIONS **1,312** CITATIONS
SEE PROFILE

Bosung Ku
Samsung Electro-Mechanics
26 PUBLICATIONS **470** CITATIONS
SEE PROFILE

Kim Sangjin
Samsung Electro-Mechanics
15 PUBLICATIONS **87** CITATIONS
SEE PROFILE

analytical chemistry

Article

pubs.acs.org/ac

High-Throughput Screening (HTS) of Anticancer Drug Efficacy on a Micropillar/Microwell Chip Platform

Dong Woo Lee,*[,†,∥] Yeon-Sook Choi,[‡,#,∥] Yun Jee Seo,[‡,#] Moo-Yeal Lee,[§] Sang Youl Jeon,[†] Bosung Ku,[†] Sangjin Kim,[†] Sang Hyun Yi,[†] and Do-Hyun Nam*[,‡,#]

[†]Central R & D Institute, Samsung Electro-mechanics Company, Ltd., 314, Maetan 3-Dong, Yeongtong-Gu, Suwon-Si, 443-743 Gyeonggi-Do, Republic of Korea

[‡]Department of Neurosurgery, Samsung Medical Center, School of Medicine, Sungkyunkwan University, 81 Irwon-Ro Gangnam-gu, 135-710 Seoul, Republic of Korea

[§]Department of Chemical and Biomedical Engineering, Cleveland State University, 2121 Euclid Ave., SH 455, Cleveland, Ohio 44115-2214, United States

[#]Samsung Biomedical Research Institute, Sungkyunkwan University School of Medicine, Seoul, 135-710, Korea

ABSTRACT: Contemporary cancer therapy refers to treatment based on genetic abnormalities found in patient's tumor. However, this approach is faced with numerous challenges, including tumor heterogeneity and molecular evolution, insufficient tumor samples available along with genetic information linking to clinical outcomes, lack of therapeutic drugs containing pharmacogenomic information, and technical limitations of rapid drug efficacy tests with insufficient quantities of primary cancer cells from patients. To address these problems and improve clinical outcomes of current personalized gene-targeted cancer therapy, we have developed a micropillar/microwell chip platform, which is ideally suited for encapsulating primary cancer cells in nanoscale spots of hydrogels on the chip, generating efficacy data with various drugs, eventually allowing for a comparison of the in vitro data obtained from the chip with clinical data as well as gene expression data. As a proof of concept in this study, we have encapsulated a U251 brain cancer cell line and three primary brain cancer cells from patients (448T, 464T, and 775T) in 30 nL droplets of alginate and then tested the therapeutic efficacy of 24 anticancer drugs by measuring their dose responses. As a result, the IC_{50} values of 24 anticancer drugs obtained from the brain cancer cells clearly showed patient cell-specific efficacy, some of which were well-correlated with their oncogene overexpression (c-Met and FGFR1) as well as the in vivo previous results of the mouse xenograft model with the three primary brain cancer cells.

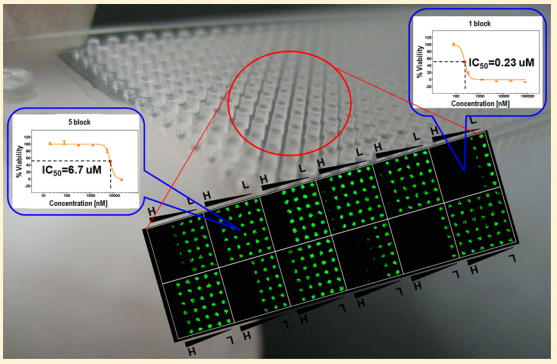

With advances in human genome analysis, researchers have discovered hundreds of new genes that are involved in human diseases, particularly cancers.[1] These newly discovered oncogenes represent powerful new drug targets, but correlating genetic mechanisms of diseases to predictive patients' therapy is still in its early stages.[2] The personalized gene-targeted cancer therapy is indeed faced with numerous challenges, which encompass tumor heterogeneity and molecular evolution, insufficient tumor samples available, along with genetic information linking to clinical outcomes, lack of therapeutic drugs containing pharmacogenomic information, and technical limitations of rapid drug efficacy tests with insufficient quantities of primary cancer cells from patients.

In an effort to address these challenges and also improve predictability of gene-targeted cancer therapy, high-throughput efficacy tests of therapeutic drugs against primary human cancer cells need to be conducted under in-vivo-like cell culture conditions such as a three-dimensional (3D) culture. Understanding behaviors of primary cancer cells from patients with individual genetic disease information at different culture conditions and finding out optimum cell culture conditions that allow primary cancer cells to maintain their in vivo physiological properties can be extremely important to better predict patient responses to therapeutic anticancer drugs. However, conventional high-throughput screening (HTS) are based on two-dimensional (2D) cell monolayer cultures commonly used in 96-well plates with liquid-dispensing and plate-handling robotics.[3] It is well-known that many cancer cells lose some of their phenotypic properties when grown in vitro as 2D monolayers over time.[4−7] The formation of tumorlike 3D structures is highly inhibited in 2D monolayer cultures due to the strong affinity of cells to most artificial surfaces and the restriction to a 2D space, severely limiting intercellular contacts and interactions. Thus, we develop a novel miniaturized 3D cell culture chip platform (micropillar/microwell chip) that can

Received: August 11, 2013
Accepted: November 7, 2013
Published: November 7, 2013

   dx.doi.org/10.1021/ac402546b | *Anal. Chem.* 2014, 86, 535−542

maintain specific biochemical and morphological features of human cancer cells similar to the corresponding tumors in vivo with a high-throughput manner.

Among various previous 3D cell culture systems, which include 96-well plates with hydrogels (e.g., alginate, matrigel, puramatrix, collagen, etc.), 3D polymer scaffolds, and hanging droplet plates,[8−14] we selected alginate as a matrix for cell encapsulation and formed a 30 nL spot on a novel chip platform (micropillar/microwell chip, see Figure 1) for the

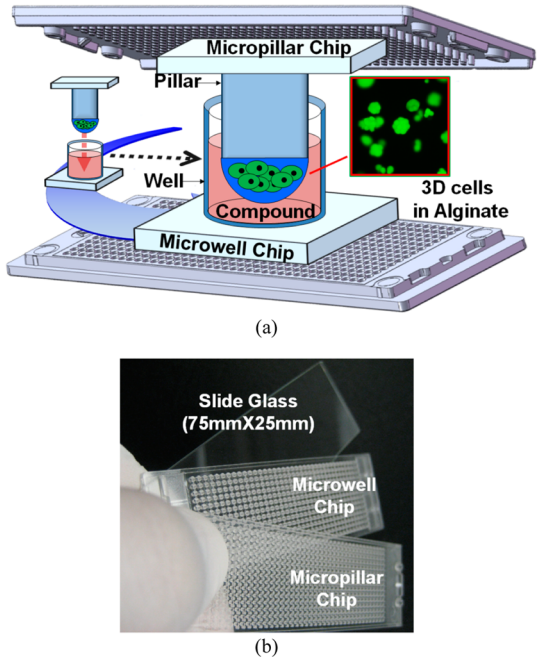

Figure 1. (a) Schematic and (b) photo of the micropillar and microwell chip platform for miniaturized 3D cell cultures.

miniaturization. In particular, because assay miniaturizations[15−20] are an important issue for 3D cell cultures, we devoted our efforts to develop miniaturized 3D cell cultures that can easily be adoptable in HTS and applicable to primary cancer cell cultures with limited amounts of tissue samples from patients. Additionally, unlike previous miniaturized 3D cell cultures in 96-well plates that require a tedious growth medium change without disturbing the cell-containing hydrogels, growth media in the micropillar/microwell chip can be replaced by simply sandwiching the cell-containing micropillar chip onto the medium-containing microwell chip. This key medium changing method can be applicable to compound exposure to cells as well as cell staining, thus allowing us to perform complicated miniaturized 3D cell-based assays in a high-throughput manner.

The miniaturized chip platform (micropillar/microwell chip) is particularly beneficial when valuable primary human cells are used for assays. In the case of testing primary cells against large combinations of therapeutic drugs, one of the key bottlenecks is limited amounts of primary cells available from noninvasive biopsy or primary cells. Therefore, assay miniaturization plays an important role in HTS of potent compounds with primary human cells. With the use of the micropillar/microwell chip platform, one of our key goals of this study is to investigate whether primary human brain cancer cells from patients show high patient variability in terms of drug efficacy according to gene expressions, which will eventually provide a valuable insight into personalized cancer therapy.

MATERIALS AND METHODS

As shown in Figure 2, the micropillar chip containing human cells in alginate was sandwiched (or "stamped") with the microwell chip for 3D cell cultures and drug efficacy tests. The micropillar chip consists of 532 pillars of 750 μm diameter, onto which 30 nL of alginate droplets of human brain tumor cells were dispensed, as shown in Figure 2a. For stabilizing cells, the micropillar-chip-containing cells is sandwiched by the complementary microwell chip that consists of 532 wells of 1.2 mm diameter, into which 950 nL of growth media (Figure 2b) were previously dispensed. After 1 day of incubation, the micropillar chip containing cells moves to a new microwell chip filled with various test drugs, and combined chips are incubated during two doubling time of cells for efficacy tests, as shown in Figure 2c. To measure cell viability, cells on the micropillar chip are stained and scanned (Figure 2d). Scanned images of the live cells (Figure 2e) were obtained by using an optical fluorescence scanner (S^+ Chip Scanner, Samsung Electro-Mechanics Company, Ltd., South Korea). Green dots represent live cells and black dots indicate dead cells. As drug dosage increases from left to right in Figure 2e, green intensity of the cell also decreases due to response of the cell to the drug. Figure 2e shows enlarged image of cells on the single micropillar. The cells grow well by forming a cell clone, which is the key characteristic of the 3D cell culture. With those images, a dose response assay was performed on the micropillar/microwell chip for determining the efficacy of 25 test drugs.

Preparation of the Micropillar and Microwell Chip. The micropillar chip and the microwell chip manufactured by plastic injection molding are a robust and flexible platform for mammalian cell culture, enzymatic reaction, viral infection, and compound screening (Figure 1). The micropillar chip made of poly(styrene-*co*-maleic anhydride) (PS-MA) contains 532 micropillars (0.75 mm pillar diameter and 1.5 mm pillar-to-pillar distance). PS-MA provides a reactive functionality to covalently attach poly-L-lysine (PLL), ultimately attaching alginate spots by ionic interactions. In addition, the microwell chip made of polystyrene (PS) has complementary 532 microwells (1.2 mm well diameter and 1.5 mm well-to-well distance). As shown in Figure 1b, both the micropillar chip and the microwell chip are similar to conventional microscopic glass slides in terms of size (75 × 25 mm). Plastic molding was performed with an injection molder (Sodic Plustech Inc.).

Cell Line and Primary Cell Cultures. With consent from patients, brain tumor samples were obtained and primary glioblastoma (GBM) cells were isolated. The characteristics of the GBM cells used in this study and isolation procedures were described in detail in our prior work.[21] A U251 brain cancer cell line and the three primary GBM cells from patients (448T, 464T, and 775T) were cultured in a CO_2 incubator (2406 CO_2 incubator, Sheldon Mfg., Inc.) at 37 °C and passaged in Neurobasal A media (Invitrogen) supplemented with B27 and N2 supplements (2-fold dilution each; Invitrogen) and recombinant bFGF and EGF (20 ng/mL each; R&D Systems).

Miniaturized 3D Cell Cultures on the Micropillar/Microwell Chip Platform. The 3D cell spots in alginate were strongly attached on the micropillar chip made of PS-MA through poly-L-lysine (PLL from Sigma-Aldrich) and barium chloride ($BaCl_2$ from Sigma-Aldrich) chemistries. PLL with amine groups were covalently attached to the maleic anhydride

dx.doi.org/10.1021/ac402546b | *Anal. Chem.* 2014, 86, 535−542

group on the PS-MA micropillar, and then negatively charged alginate was gelled by $BaCl_2$ and attached to positively charged PLL by an ionic interaction. Briefly, as shown in Figure 2a, 60

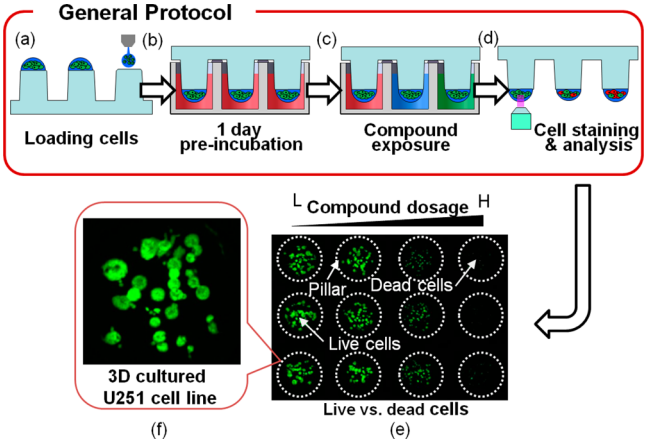

Figure 2. Experimental protocols for drug efficacy testing: (a) dispensing cells in alginate on the top of PLL/$BaCl_2$ bottom layers on the micropillars, (b) immersing cells in the microwells containing growth media to maintain high cell viability, (c) dispensing drugs into the microwells and exposing cells to drugs by sandwiching two chips together, (d) staining cells with calcein AM and scanning the micropillar chip for data analysis, (e) analyzing scanned images with live and dead cells at different drug dosages, and (f) a blown-up image of 3D-cultured U251 cells in 30 nL of an alginate spot after drying the spot.

nL of PLL at a concentration of 0.01 wt %/vol was dispensed on the top of the pillar surface by using a microarray spotter (Samsung Electro-Mechanics Company, Ltd., South Korea). Immediately after spotting, the micropillar chip with PLL was placed in a humid incubation chamber (Figure 3a) for 1 h to

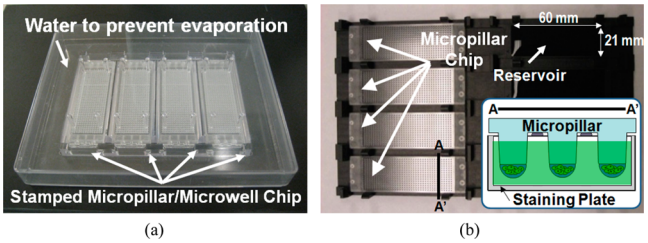

Figure 3. Apparatuses for the micropillar/microwell chip platform: (a) gas-permeable incubation chamber for cell cultures on the chip and (b) deep/shallow staining plate with 8 wells for cell washing/staining.

prevent water evaporation and ensure covalent attachment of PLL on the PS-MA surface. Followed by washing PLL with Dulbecco's phosphate-buffered saline (DPBS from Invitrogen) and drying the micropillar chip at room temperature for 2 h, 60 nL of $BaCl_2$ (Sigma-Aldrich) at a concentration of 0.02 M was dispensed on the PLL-coated micropillar and then the chip was dried overnight at room temperature. To encapsulate GBM cells in alginate on the chip, 30 nL of cell suspension in 0.5% alginate was dispensed on the PLL/$BaCl_2$-coated micropillar chip (Figure 2a). While spotting cells, the micropillar chip was placed on a chilling slide deck at 12 °C to retard evaporation of water in the spots. The suspension of GBM cells in low-viscosity alginate (Sigma-Aldrich) was prepared by mixing 300 μL of the cell suspension in the culture medium (6×10^6 cells/mL) with 100 μL of 3% alginate in distilled water and 200 μL of the culture medium so that the final concentration of the GBM cells and alginate were 3×10^6 cells/mL and 0.5% (wt/vol), respectively. After approximately 2 min of gelation, the cell spots on the 532 micropillars were immersed in 950 nL of the culture medium in the complementary 532 microwells by sandwiching two chips together ("stamping"). The stamped micropillar chip onto the microwell chip was placed in a gas-permeable incubation chamber (Figure 3a) and then incubated in the CO_2 incubator at 37 °C for 24 h prior to efficacy tests (Figure 2b).

Drug Efficacy Tests on the Micropillar/Microwell Chip Platform. High-throughput screening of anticancer drug efficacy on miniaturized cell arrays were performed by dispensing therapeutic drugs into the microwell chip and then sandwiching ("stamping") the micropillar chip with the cells onto the microwell chip (Figure 2c). For the efficacy screening, 25 different therapeutic drugs, including cisplatin, a receptor tyrosine kinase (RTK) inhibitor targeting FGFR, c-Met, EGFR, and VEGFR, as well as docetaxel, a chemotherapy drug, were selected. Drug stock solutions were prepared by dissolving the drugs in DMSO. Typically, higher than 100 mM of drug stock solutions were prepared to maintain final DMSO content less than 0.5%. Approximately 40 μL of drug stock solutions were prepared at 200-fold higher concentrations than the desired final concentration (5 dosages plus 1 control) by serial dilutions of drug stock solutions in DMSO in a 384-well plate. As a control, 100% DMSO without the drug was used. After that, 300 μL of diluted drug solutions in a round-bottom 96-well plate were prepared by mixing 1.5 μL of the diluted drugs in DMSO with 298.5 μL of the culture medium (typically 0−1000 μM of final concentrations). By using the microarray spotter, 950 nL of the diluted drug solutions in the growth medium were dispensed onto the microwell chip. Twelve different drugs were dispensed in regions 1−12 on the microwell chip, each region containing a 6 × 6 mini-array (Figure 4). Within each mini-array, 6 different doses of a drug

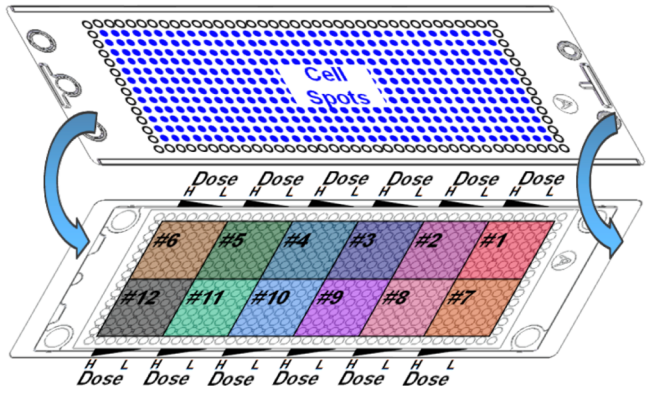

Figure 4. Layout of the micropillar/microwell chip for screening 12 drugs per chip.

(5 dosages plus 1 control) were assayed for efficacy. The same volume of the growth medium without the drug was printed into microwells located in the periphery of the microwell chip (i.e., sacrificial regions) to avoid edge-drying issues during incubation.

After taking out the preincubated micropillar and microwell chip from the gas-permeable chamber, the microwell chip with the culture medium was separated and discarded, and then the

dx.doi.org/10.1021/ac402546b | Anal. Chem. 2014, 86, 535−542

micropillar chip was stamped on the top of a new microwell chip with 12 drugs by aligning the edges of the chips, thus exposing cells to drugs (Figure 2c). The stamped chips were placed in the gas-permeable chamber with 20 mL of sterile distilled water to prevent water evaporation during incubation and then incubated for up to two doubling time in the CO_2 incubator at 37 °C for drug efficacy tests. During the drug exposure, there was no growth medium changed. In addition, the drug exposure time was determined based on the doubling time of the cells. Basically, we incubated the cells with the drugs for a period of approximately 2 doubling times. For example, for 464T cells with an approximately 3-day doubling time, the cells were exposed to the drugs for 6 days.

Cell Staining and Chip Scanning. At the end of the incubation, the cells were stained with calcein AM (Figure 2d), which can be transported through the cellular membrane and can produce a green fluorescence response from living cells, making it useful for testing cell viability. As the schematic shown in Figure 3b, all 532 micropillars on the micropillar chip separated from the microwell chip were immersed into a large reservoir (60 × 21 mm) containing buffer solutions or fluorescent dyes for cell washing and cell staining on the staining plate. In accordance with the depth of the reservoir, the shallow-staining plate has a 2 mm depth for cell staining and the dip staining plate has a 5 mm depth for washing before and after staining. For cell washing, a deep (5 mm in depth) staining plate, accommodating 5−6 mL of buffer solution per reservoir, was used, whereas a shallow (2 mm in depth) staining plate accommodating 1.5−2 mL dye solution per reservoir was used for cell staining. The micropillar chip was washed twice for 5 min each by immersing micropillars with cell spots in the deep staining plate, containing 5 mL of 140 mM NaCl with 20 mM $CaCl_2$. $CaCl_2$ was supplemented to prevent degradation of alginate spots during washing. A staining dye solution was prepared by adding 1.0 μL of calcein AM (4 mM stock from Invitrogen) in 8 mL of 140 mM NaCl supplemented with 20 mM $CaCl_2$. To stain the cell spots, 2 mL of the dye solution was dispensed in the shallow staining plate and then the micropillar chip was placed on the top of the shallow staining plate (Figure 3b). Followed by incubating the micropillar chip in the dark for 45 min at room temperature, the micropillar chip was washed twice for 15 min each by immersing it with cell spots in the dip staining plate containing 5 mL of 140 mM NaCl with 20 mM $CaCl_2$ to remove excess dye in the alginate spots. After drying the micropillar chip in the dark for at least 2 h, the location of each cell spot exposed to a drug was detected by imaging the entire micropillar chip using S^+ Chip Scanner (Samsung Electro-Mechanics Company, Ltd., South Korea) equipped with a mercury light source (Olympus U-RFL-T), a ccd camera (Point Gray), 4× and 10× objective lenses (Olympus UPlanFLM) and excitation/emission filters (Thorlab) (Figure 2d). An excitation filter of 475 ± 35 nm and an emission filter of 530 ± 43 nm which are optimum for detecting green fluorescence from live cells stained with calcein AM were used. The microscope on a moving stage in the scanner automatically focused on cell spots by moving in the z direction, and selecting the highest fluorescent cell image, took 532 individual pictures from a single stained micropillar chip at a 4× magnification. The 532 pictures of cell spots were then consolidated into a single JPEG image for data analysis (Figure 6). From the image of the cell spots, the green fluorescent intensity from live cells in each spot was extracted using the S^+ Chip Analyzer (Samsung Electro-Mechanics Company, Ltd., South Korea). The software extracted mean green fluorescent intensities (8 bit Green code among RGB code: 0−255) from living cells in each cell spot on the scanned chip by setting up an analysis boundary (Figure 2e), plotted sigmoidal dose response curves with the percentage of live cells against the concentration of the test compound (green intensity in no drug condition is 100%), and then calculated IC_{50} values for each test drug.

Data Analysis for the Dose Response Assay. A dose response curve is generally characterized by a nonlinear relationship between the biological response and the amount of a drug given. The biological responses in our case were measured by fluorescent intensities from cell spots, which were linearly proportional to the number of live cells in each spot. The green fluorescent intensity was extracted from each cell spot, and then the percentage of live cells was plotted against the concentration of the drug tested. The percentage of live cells was calculated using the following equation:

$$\%\ \text{live cells} = \frac{F_{\text{drug}}}{F_{\text{max}}} \times 100 \tag{1}$$

where F_{drug} is the green fluorescent intensity of the cell spot exposed to a drug and F_{max} is the green fluorescent intensity of untreated viable cells. To produce a conventional sigmoidal dose response curve, with response values normalized to span the range from 0% to 100% plotted against the logarithm of the test concentration, the green fluorescent intensities of all cell spots were normalized with the fluorescent intensity of the 100% live cell spot (i.e., cell spots contacted with no drug) and the test drug concentration was converted to their respective logarithms. The sigmoidal dose response curves (variable slope) and IC_{50} values (i.e., concentration of the drug where 50% of cell growth inhibited) were obtained using the following equation:

$$Y = \text{bottom} + \left[\frac{\text{top} - \text{bottom}}{1 + 10^{(\log \text{IC}_{50} - X) \times H}}\right] \tag{2}$$

where IC_{50} is the midpoint of the curve, H is the hill slope, X is the logarithm of the test concentration, and Y is the response (% live cells), starting at bottom and going to top with a sigmoid shape.

Gene Expression Analysis of Primary GBM Cells. Of the three primary GBM cells used in the study, gene expression for two (464T and 448T) were measured in our previous study,[21] and the data were downloaded from the Gene Expression Omnibus (GSE42670). For 775T primary cells, the gene expression microarray experiment was conducted using Affymetrix Human Gene 1.0 ST array, as described in Joo et al.[21]

RESULTS AND DISCUSSION

3D Cell Cultures in Alginate Spots on the Micropillar Chip. On the micropillar/microwell chip, a U251 brain tumor cell line and three primary GBM cells (464T, 448T, and 775T) were cultured in 3D alginate spots as small as 30 nL. As the final concentration of the cells in the mixture of the cells and alginate was 3 × 10^6 cells/mL, the calculated number of the cells spotted on each pillar was 90 in a 30 nL droplet. Because of the relatively hydrophobic nature of the micropillar surface, the cell spots formed a hemispherical shape after dispensing and then quickly formed a gel. Therefore, we were able to estimate its thickness from a simple mathematical equation.

dx.doi.org/10.1021/ac402546b | Anal. Chem. 2014, 86, 535−542

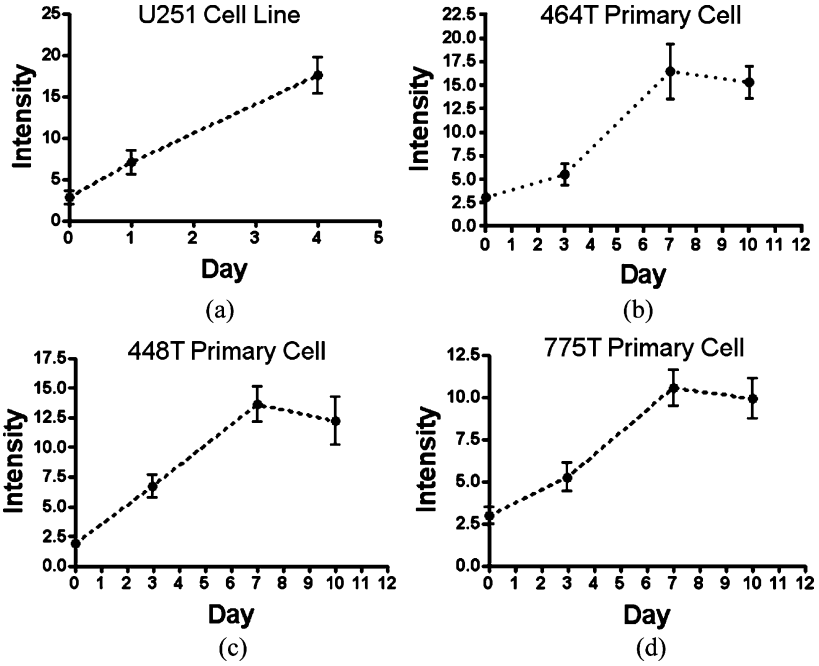

Figure 5. Growth curves of 3D cultured cells on the chip: (a) U251 cell line, (b) 464T cells, (c) 448T cells, and (d) 775T cells, where the last three cell types were from patients.

The calculated thickness of 30 nL cell spots at the tip of the micropillar is approximately 242 μm. Measuring the thickness of the wet alginate spots on the micropillar was difficult. However, the cell spots on the micropillar chip were very uniform in terms of their shape and the cell number under the microscope. For 72 spots with theoretical 90 cells per micropillar (i.e., 30 nL of cell spots at 3×10^6 cell seeding/mL), the average number of the cells in the spot measured was 82 $\pm$ 9 under the microscope. The uniformity of cell distribution in spots was under approximately 20%.

Interestingly, a unique 3D morphology of U251 cells in 30 nL of alginate spots was observed approximately 4 days after the cell culture. U251 cells on the chip formed spherical shapes over time, which are general characteristics of 3D cell cultures (Figure 2f), whereas U251 cell monolayer in T75 flasks showed traditional elongated shapes. The three primary GBM cells also grew well on the micropillar/microwell chip platform and formed 3D spherical shapes over time. From our microscopic observation with the 3D cultured cells, we noticed that the three primary GBM cells grown on the chip formed a round shape, tight single 3D colony, whereas the 3D suspension culture counterpart formed aggregates of many single cells, which is completely different from the morphology of brain tumors in vivo. As the chip imaging system detected the green fluorescent cells in the dried spots, the thickness did not affect imaging. However, when wet cell spots were imaged, we observed some cell colonies out of focus due to randomly distributed 3D spherical cells in alginate spots. The growth curves of U251 cells and the three primary GBM cells (464T, 448T, and 775T) were shown in Figure 5. The intensities of green dots representative of live cell aggregates, forming 3D structures, increased over time, which indicated that all cells tested on the chip grew well. The population of cells in replicates of the spots over time was uniform within approximately 20% of the error ranges (Figure 5). As expected, the U251 cell line grew the fastest, and 775T cells grew the slowest. The doubling times of each cell were calculated from its growth curve (Table 1) by the following equation.

$$\text{doubling time} = (T_2 - T_1)/\ln\left(\frac{I_2}{I_1}\right) \quad (3)$$

where I_1 and I_2 are the green intensities at the times of T_1 and T_2, respectively.

Table 1. Calculated Doubling Time (h) of the 3D-Cultured Cells on the Micropillar/Microwell Chip as well as the 2D-Cultured Counterpart in the 96-Well Plate

	brain cancer cell line		primary brain cancer cells from patients		
	U251		775T	448T	464T
	3D	2D	3D	3D	3D
doubling time (h)	36	21	92	57	69

The doubling time of U251 cells was calculated within 0−4 days of the culture period due to relatively fast growth rates, whereas the double times of the three primary GBM cells were calculated within 0−7 days. As a result, the double times of the U251 cell line in 3D and 2D systems were 36 and 21 h, respectively. In the case of the three primary GBM cells, the cells grew very slowly, and the growth rates were rapidly decreased after 7 days of the culture period, presumably due to the limited amount of nutrients supporting large cell colonies. From these doubling times for each cell type, 3 days of drug exposure for the U251 cell line and 6 days of drug exposure for the three primary GBM cells were determined.

Patient Cell-Specific Responses of Therapeutic Drugs. With 6 dosages per drug, the dose response curves and corresponding IC_{50} values were calculated from the scanned images using the S^+ Chip Analyzer (Samsung Electro-Mechanics Company, Ltd., South Korea). Twelve dose response curves with 6 dosages and 12 IC_{50} values were

dx.doi.org/10.1021/ac402546b | Anal. Chem. 2014, 86, 535−542

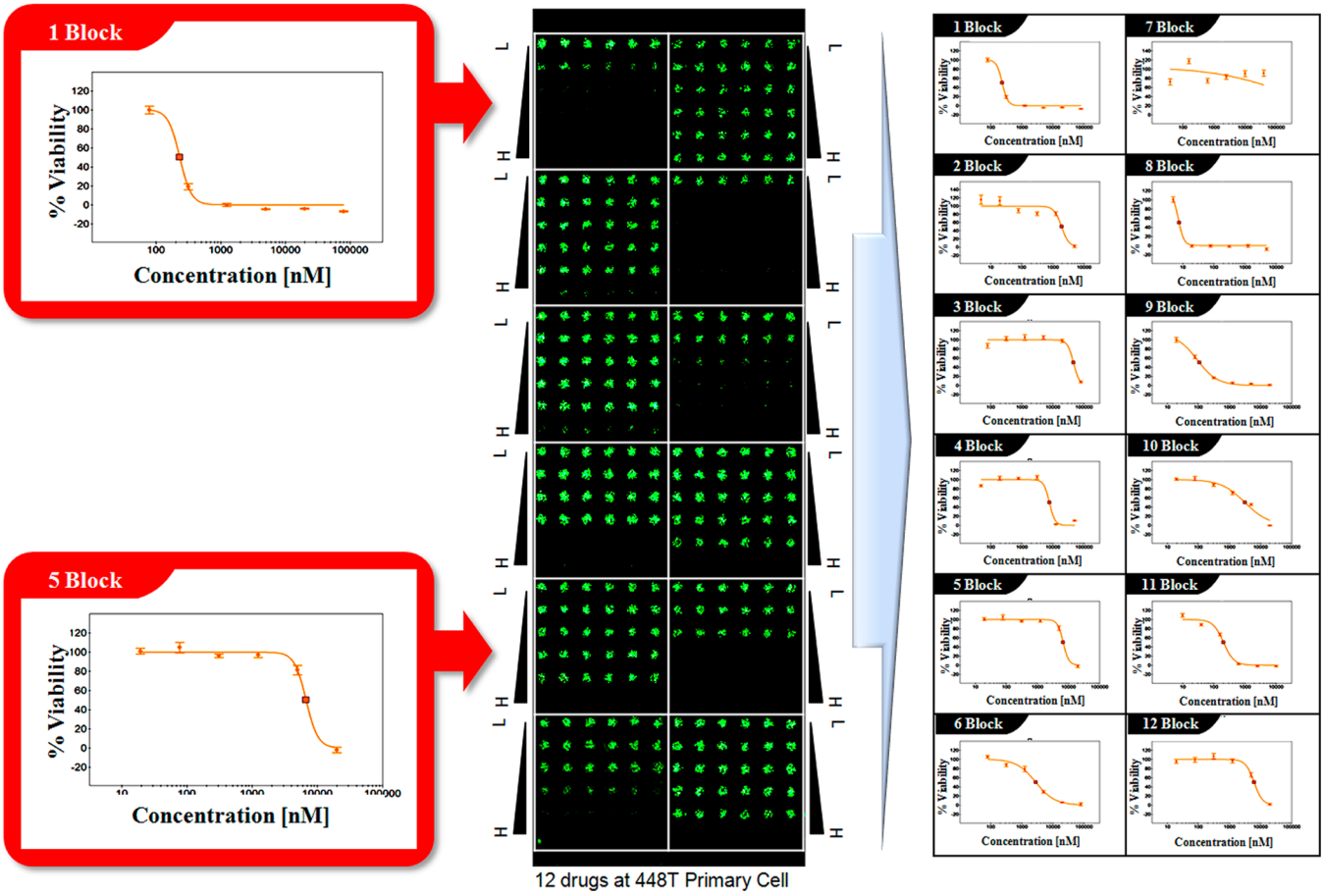

Figure 6. Scanned image of a single micropillar chip exposed to 12 drugs, each drug with 6 dosages, and obtained dose 12 response curves and their corresponding IC_{50} values.

obtained from a single scanned image of the micropillar chip (Figure 6). Twenty-four drugs were tested against a U251 brain cancer cell line, and 25 drugs were tested against brain cancer cells from patients (448T, 464T, and 775T) on the micropillar/microwell chip. As a result, the efficacy of drugs against the U251 brain cancer cell line and the three primary brain cancer cells from patients were summarized in Table 2. To study the effectiveness of the 3D cultured human cells on the micropillar/microwell chip for efficacy tests, IC_{50} values of the 24 anticancer drugs against the 3D-cultured U251 cell line were compared with those from the 2D-cultured counterpart in 96-well plates. For the 2D tests, 500 of U251 cells were seeded in each 96 well, cultured for 24 h, and then exposed to 100 μL of drug solutions in the growth medium for 3 days. Followed by drug treatment, 10 μL of CCK-8 solution (Dojindo Molecular Technologies, Kumamoto, Japan) was added into each 96 well to measure cell viability and calculate IC_{50} values of test drugs. In general, the IC_{50} values of 24 drugs tested against the U251 cell line on the chip were substantially similar to those obtained from its 2D counterpart in 96-well plates except for 2 drugs. Interestingly, IC_{50} values of HK1−272 and Geldanamycin obtained from the 3D culture on the chip were about 10 times higher than those from the 2D counterpart. This kind of disparity on IC_{50} values between 3D and 2D cell-culture systems has already been reported in some literature and is considered a distinctive characteristic of cells cultured in 3D systems.[9,10] We hypothesized that the expression of phenotypic proteins/genes and the formation of in vivo tumorlike morphology facilitated by cell−cell or cell−extracellular matrix (ECM) interactions in the 3D cell-culture system are responsible for significant differences in IC_{50} values.

With the robust assay, we developed on the chip for efficacy tests, we also examined responsiveness of the 24 anticancer drugs against the three patient GBM cells. Temozolomide (TMZ) was additionally included as a standard drug. As a result, the efficacy of the 25 anticancer drugs on the patient GBM cells varied dramatically, depending on their target gene expression, in some cases over 100 folds. As shown in Figure 7, the c-Met gene was overexpressed in 775T cells and the FGFR1 gene was overexpressed in 448T cells. Interestingly, as shown in Table 2, c-Met inhibitors (PHA665752 and SU11274)[22] and the FGFR inhibitor (PD173074)[23] strongly suppressed the growth of 775T and 448T cells, respectively, which was consistent with their sensitive response to oncogene expression from the three primary GBM cells.

TMZ treatment is widely used for GBM patients, and its sensitivity in GBM tumors is associated with the O6-methylguanine−DNA methyl transferase (MGMT) methylation status.[24] The MGMT methylation status of the 2 GBM cells (464T and 448T cells) from the GBM patients and mouse tests were obtained in our previous work.[21] Thus, we examined the responses to TMZ among the 3 GBM cells on the chip. As a result, MGMT-methylated 464T cells were significantly more responsive to TMZ (IC_{50} = 21.6 μM) compared with MGMT-unmethylated 448T cells (IC_{50} > 1000 μM), which was well-correlated with the results from mouse tests.[21]

dx.doi.org/10.1021/ac402546b | Anal. Chem. 2014, 86, 535−542

Table 2. IC_{50} Values (nM) of 24 Anticancer Drugs Obtained from the 3D-Cultured Cells on the Micropillar/Microwell Chip as well as the 2D-Cultured Counterpart in the 96-Well Plate

			brain cancer cell line		primary brain cancer cells from patients		
			U251		775T	448T	464T
drug		target	3D[a]	2D	3D[a]	3D[a]	3D[a]
1	CI-1040	Mek	3050	5600	250	210	1665
2	BIBW 2992	HER2/EGFR	>5000	>5000	480	2000	310
3	PLX4720	BRAF	18500	16000	37000	45000	18000
4	PHA665752	c-Met	12750	3900	130	8150	6600
5	HKI-272	HER2/EGFR	7700	810	490	7100	4300
6	Dasatinib	Src/c-kit	2100	1200	730	3100	2100
7	Gö 6976	PKC	>40000	>40000	490	>40000	11000
8	Geldanamycin	Hsp90	185	13	8.15	7.4	8.2
9	AZ628	BRAF/CRAF	2150	1000	130	105	1350
10	Sorafenib	PDGFR/KDR	1600	3400	6100	3450	3300
11	Vandetanib	EGFR/KDR	175	130	315	180	190
12	TAE684	ALK	1200	690	1845	4950	1750
13	PD173074	FGFR	6200	7100	2150	47.5	2400
14	AZD0530	Src/Abl	3250	6400	6800	>20000	9650
15	SU11274	c-Met	58000	4900	380	12500	5800
16	U0126	MEK	55000	47000	5100	7500	8950
17	Docetaxel	Tublin	11.9	5.8	0.95	32	0.85
18	Erlotinib	EGFR	8250	5000	370	10400	1250
19	Gefitinib	EGFR	>5000	>5000	>5000	>5000	>2000
20	Cisplatin	DNA synthesis	>20000	>20000	>2000	>2000	>2000
21	Purvalanol A	CDK1	10600	6900	4850	7700	3900
22	Sunitinib malate	PDGFR/KDR	2800	1400	1450	7300	6300
23	17-AAG	Hsp90	350	190	975	160	170
24	Rapamycin	mTOR	455	1000	1250	1650	950
25	TMZ	MGMT	–	–	12650	$>1\times10^6$	21580

[a]Standard deviations are less than 1 dose (3 times the drug serial dilution ratio).

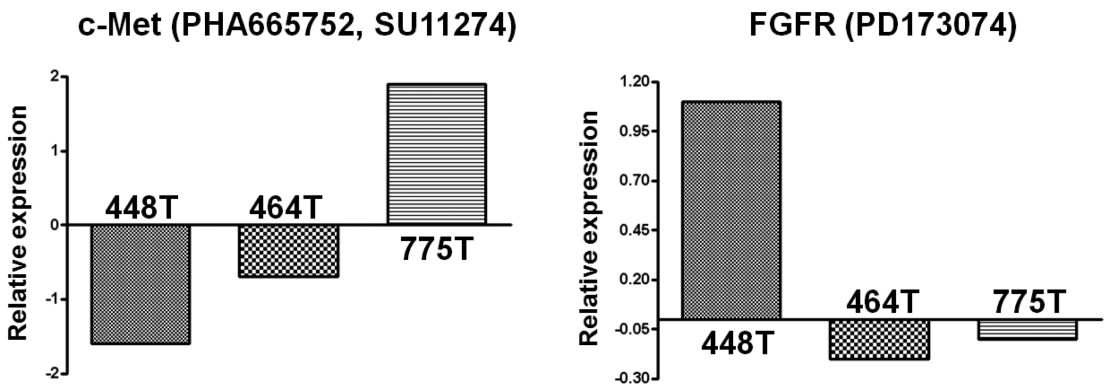

Figure 7. Expression levels of (a) c-Met and (b) FGFR1 genes in 448T, 464T, and 775T cells.

CONCLUSION

The micropillar/microwell chip platform has been developed to facilitate miniaturized 3D cell cultures and perform high-throughput, biochemical and cell-based assays. To demonstrate its capability for 3D cell cultures in the microenvironment and cell-based efficacy assays, we cultured the U251 brain cancer cell line and the three primary brain cancer cells from patients on the chip and performed a dose response assay with the 24 therapeutic anticancer drugs. As a result, we were able to observe patient cell-specific responses to some drugs in 3D-cultured cells on the chip. The low IC_{50} values obtained from the 775T cells exposed to PHA665752 and SU11274 might be a result of their high expression level of c-Met gene in the 3D-cultured 775T cells. It is well-known that both PHA665752 and SU11274 are targeting the c-Met gene in brain cancer cells. Similar results were obtained for the 448T cells exposed to PD173074, which is known to target the FGFR1 gene. Therefore, the chip platform has potential to predict likely drug responses from overexpressed oncogenes. In addition, the 3D chip data of the U251 brain cancer cell line were comparable to the 2D data from the 96-well plates. These results indicate that the micropillar/microwell chip platform represents a promising, high-throughput, and microscale alternative to conventional in vitro multiwell plate platforms and creates new opportunities for rapid and inexpensive assessment of drug efficacy at very early phases of clinical study for individual cancer patients. Culturing human primary cells from patients in more in-vivo-like 3D microenvironments

dx.doi.org/10.1021/ac402546b | Anal. Chem. 2014, 86, 535−542

can potentially provide a valuable insight into in vivo drug efficacy as 3D cell cultures can maintain specific biochemical and morphological features of human cells similar to the corresponding tumors in vivo. To facilitate 3D cell cultures with primary cells and mimic in vivo tumor microenvironments, a variety of cell culture methods, including gel matrices, polymer scaffolds, and hanging droplet plates, have been developed. However, none of the aforementioned techniques is ideally suited for miniaturized 3D cell cultures with valuable human cells such as primary cells freshly isolated from tissues or patient' tumors.

AUTHOR INFORMATION

Corresponding Authors

*E-mail: dw2010.lee@gmail.com.

*E-mail: nsnam@skku.edu.

Author Contributions

[‖]D.W. Lee and Y.-S. Choi contributed equally to this work.

Notes

The authors declare no competing financial interest.

ACKNOWLEDGMENTS

This study was supported by a grant from the Korea Healthcare Technology R&D Project, Ministry for Health & Welfare Affairs, Republic of Korea (Grant A092255) and a Samsung Medical Center grant [GFO1130011].

REFERENCES

(1) Hamburg, M. A.; Collins, F. S. *N. Engl. J. Med.* **2010**, *363* (4), 301−304.

(2) Butcher, E. C.; Berg, E. L.; Kunkel, E. J. *Nat. Biotechnol.* **2004**, *22* (10), 1253−1259.

(3) Shoemaker, R. H. *Nat. Rev. Cancer* **2006**, *6*, 813−823.

(4) Pampaloni, F.; Reynaud, E. G.; Stelzer, E. H. K. *Nat. Rev. Mol. Cell Biol.* **2007**, *8*, 839−845.

(5) Kenneth, M. Y.; Edna, C. *Cell* **2007**, *130*, 601−610.

(6) Kwon, C. H.; Wheeldon, I.; Kachouie, N. N.; Lee, S. H.; Bae, H.; Sant, S.; Fukuda, J.; Kang, J. W.; Khademhosseini, A. *Anal. Chem.* **2011**, *83* (11), 4118−4125.

(7) Lee, J.; Cuddihy, M. J.; Kotov, N. A. *Tissue Eng., Part B* **2008**, *14*, 61−86.

(8) Gurski, L. A.; Petrelli, N. J.; Jia, X.; Frarach-Carson, M. C. *Oncology Issues* **2010**, *January/February*, 20−25.

(9) Wong, H. L.; Wang, M. X.; Cheung, P. T.; Yao, K. M.; Chan, B. P. *Biomaterials* **2007**, *28*, 5369−5380.

(10) Wu, M.-H.; Chang, Y.-H.; Liu, Y.-T.; Chen, Y.-M.; Wang, S.-S.; Wang, H.-Y.; Lai, C.-S.; Pan, T.-M. *Sens. Actuatators, B* **2011**, *155*, 397−407.

(11) Gurski, L. A.; Jha, A. K.; Zhang, C.; Jia, X.; Farach-Carson, M. C. *Biomaterials* **2009**, *30*, 6076−6085.

(12) Deligkaris, K.; Tadele, T. S.; Olthuis, W.; van den Berg, A. *Sens. Actuatators, B* **2010**, *147*, 765−774.

(13) Horning, J. L.; Sahoo, S. K.; Vijayaraghavalu, S.; Dimitrijevic, S.; Vasir, J. K.; Jain, T. K.; Panda, A. K.; Labhasetwar, V. *Mol. Pharm.* **2008**, *5*, 849−862.

(14) Beningo, K. A.; Dembo, M.; Wang, Y. L. *Proc. Natl. Acad. Sci. U.S.A.* **2004**, *101*, 18024−18029.

(15) Lee, M.-Y.; Kumar, R. A.; Sukumaran, S. M.; Hogg, M. G.; Clark, D. S.; Dordick, J. S. *Proc. Natl. Acad. Sci. U.S.A.* **2008**, *105*, 59−63.

(16) Fernandes, T. G.; Kwon, S.-J.; Lee, M.-Y.; Clark, D. S.; Cabral, J. M. S.; Dordick, J. S. *Anal. Chem.* **2008**, *80*, 6633−6639.

(17) Lee, D. W.; Yi, S. H.; Jeong, S. H.; Ku, B.; Kim, J.; Lee, M.-Y. *Sens. Actuators, B* **2013**, *177*, 78−85.

(18) Friedrich, J.; Seidel, C.; Ebner, R.; Kunz-Schughart, L. A. *Nat. Protoc.* **2009**, *4*, 309 −324.

(19) Tung, Y. C.; Hsiao, A. Y.; Allen, S. G.; Torisawa, Y. S.; Ho, M.; Takayama, S. *Analyst* **2011**, *136* (3), 473−478.

(20) Lai, Y.; Asthana, A.; Kisaalita, W. S. *Drug Discovery Today* **2011**, *16* (7−8), 293−297.

(21) Joo, K. M.; Kim, J.; Jin, J.; Kim, M.; Seol, H. J.; Muradov, J.; Yang, H.; Choi, Y. L.; Park, W. Y.; Kong, D. S.; Lee, J. I.; Ko, Y. H.; Woo, H. G.; Lee, J.; Kim, S.; Nam, D. H. *Cell Rep.* **2013**, *3*, 260−273.

(22) Peruzzi, B.; Bottaro, D.P . *Clin. Cancer Res.* **2006**, *12* (12), 3657−3660.

(23) Loilome, W.; Joshi, A. D.; ap Rhys, C. M.; Piccirillo, S.; Vescovi, A. L.; Gallia, G. L.; Riggins, G. J. *J. Neuro-Oncol.* **2009**, *94* (3), 359−366.

(24) Hegi, M. E.; Diserens, A. C.; Gorlia, T.; Hamou, M. F.; de Tribolet, N.; Weller, M.; Kros, J. M.; Hainfellner, J. A.; Mason, W.; Mariani, L.; Bromberg, J. E.; Hau, P.; Mirimanoff, R. O.; Cairncross, J. G.; Janzer, R. C.; Stupp, R. *N. Engl. J. Med.* **2005**, *352*, 997−1003.